Heterogeneous pyrolysis: a route for epitaxial growth of hBN atomic layers on copper using separate boron and nitrogen precursors

Gene Siegel,[1] Cristian V. Ciobanu,[2*] Badri Narayanan,[3] Michael Snure,[1*] and Stefan C. Badescu[1]

[1]*Air Force Research Laboratory, Wright-Patterson AFB, Ohio 45433, USA*

[2]*Department of Mechanical Engineering and Materials Science Program, Colorado School of Mines, Golden, Colorado 80401, USA*
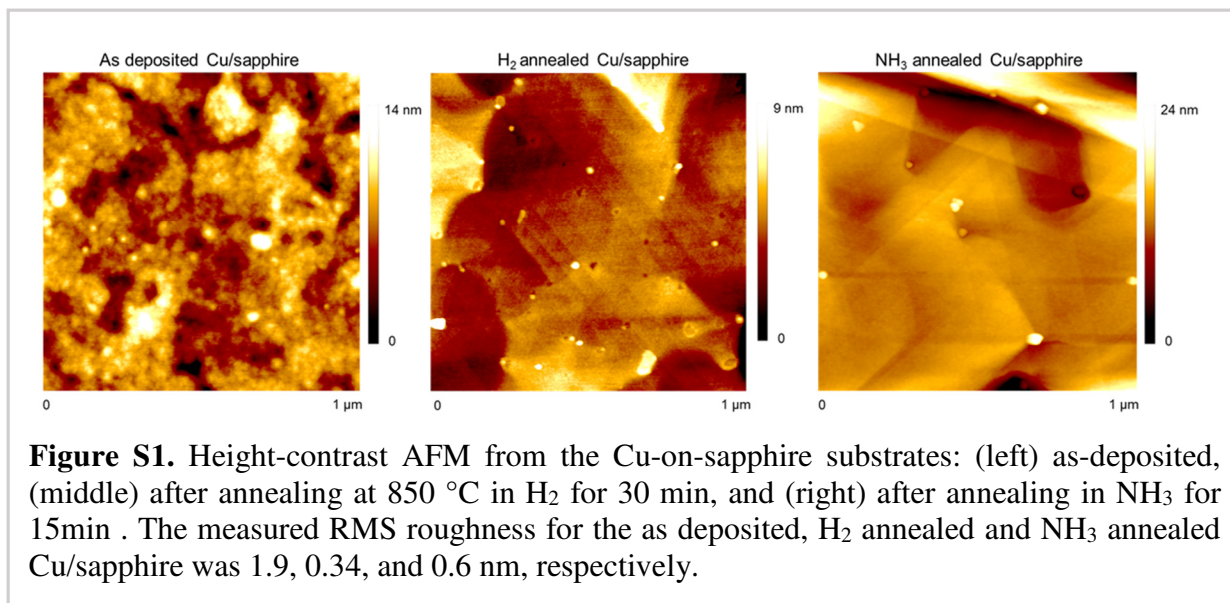
[3]*Center for Nanoscale Materials, Argonne National Laboratory, Argonne, Illinois 60439, USA*

The following contains additional information regarding growth procedure, AFM images showing the growth of the second hBN layer, Raman and AFM characterization of multilayer hBN films, and thermodynamic arguments in favor of six-atom ring formation.

_____

[*] To whom correspondence may be addressed: Cristian V. Ciobanu (cciobanu@mines.edu), Michael Snure (michael.snure.1@us.af.mil)

1. Further details regarding growth and characterization methods

hBN layers were grown in a low-pressure MOCVD reactor with an actively cooled close-coupled showerhead (CCS) at 20 Torr from Triethylboron (TEB) and NH_3. The CCS shower head design allows for separate injection of the cooled (50 °C) TEB and NH_3 precursors until just above (11 mm) the heat substrate carrier as shown in the main text. The Cu (111)/sapphire substrates were prepared by sputtering 500 nm of Cu on epi-ready c-plane sapphire substrates at 250 W in 3 mTorr of Ar at 100 °C. As deposited Cu films are (111) oriented with a typical RMF roughness of ~2 nm (Fig. SI-1). Prior to loading for h-BN growth the Cu/sapphire substrates are degreased then etched in acetic acid to remove contamination and oxides. Substrates are heated to 850 °C and annealed for 30 min in palladium purified H_2 to improve surface morphology and remove any residual oxide. After annealing, the substrates are heated to a growth temperature of 950 °C followed by NH_3 and
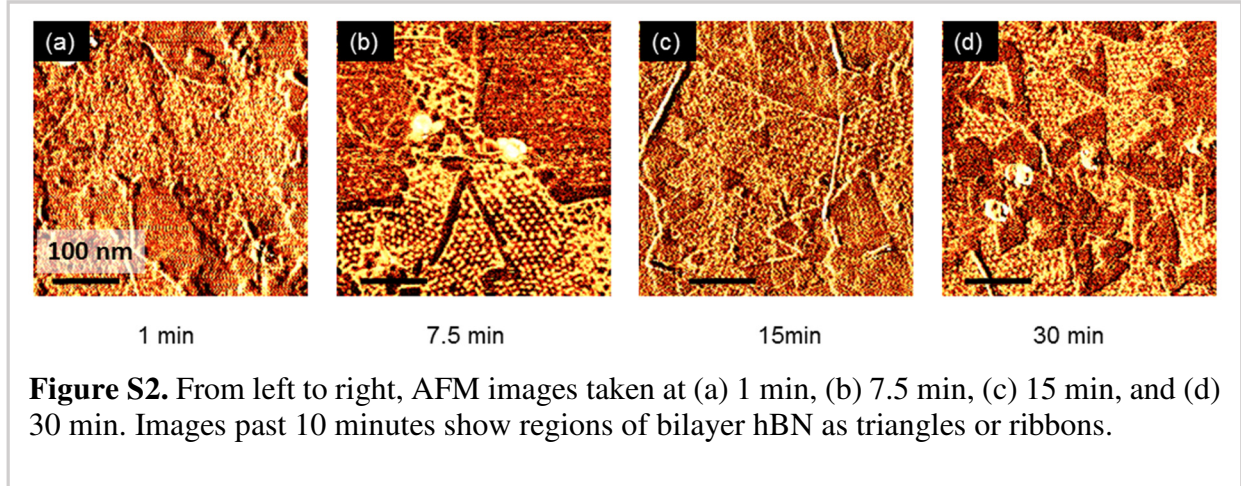

Figure S1. Height-contrast AFM from the Cu-on-sapphire substrates: (left) as-deposited, (middle) after annealing at 850 °C in H_2 for 30 min, and (right) after annealing in NH_3 for 15min . The measured RMS roughness for the as deposited, H_2 annealed and NH_3 annealed Cu/sapphire was 1.9, 0.34, and 0.6 nm, respectively.

TEB injection. A V/III ratio of 1250 was used at a total flow rate of 3 slm with 250 sccm of NH_3, 10 µmol/min of TEB and balance H_2. After growth the samples were cooled in NH_3 and H_2 down to 700 °C then cooled to room temperature in H_2.

Surface topography of the hBN films was analyzed by atomic force microscopy (AFM) using a Bruker Dimension Fast Scan in tapping mode (soft tap). Standard TESPA-V2 tips used with the Icon tip mount were utilized in collecting the data. The data collection itself was tuned such that the moiré patterns appeared most strongly and clearly. This was done by reducing the Z-height of the tip, configuring the gains for optimal tracking, and adjusting the amplitude set point just below the threshold of loss of signal. Data was collected over 1 µm × 1 µm areas at a set scan rate of 1 Hz (2 µm/sec) with 512 × 512 data points. High resolution scans were done over 250 nm × 250 nm areas at 1 Hz (500 nm/sec) also using a 512 × 512 collection grid. X-ray photoelectron spectroscopy (XPS) was used to characterize the chemical composition and bonding environment of films using a PHI (Perkin-Elmer) 55000 XPS with an Al K_α X-ray source. Raman spectroscopy was used to identify the bonding nature of BN using a Renishaw inVia system. An accumulation of 120 scans, each of 30-second duration, was collected using a 4 mW 488nm excitation source, 20-µm slits and 3000 line/mm grating for each measurement. For Raman characterization films were transferred from the Cu/sapphire substrates to 300 nm thick SiO_2 on Si handle substrates. A

PMMA layer was coated onto the hBN film, and then the Cu was dissolved in 0.1 M ammonium persulfate, the PMMA/BN stack was then rinsed in DI water, and transferred to the SiO_2/Si substrate. PMMA was removed by dissolving in acetone at 55 °C. Results from these characterization methods have been included in Figure 1 of the main text.

2. Time-lapse AFM images showing details of growth of the second hBN layer

We have performed growth for specific durations, and then characterized the samples using AFM. Typical results are shown in Figure S2.

Figure S2. From left to right, AFM images taken at (a) 1 min, (b) 7.5 min, (c) 15 min, and (d) 30 min. Images past 10 minutes show regions of bilayer hBN as triangles or ribbons.

3. Characterization of multi-layer hBN films

Additional Raman and AFM characterization of hBN grown for 60 min is shown in Figure S3. Raman shows only peaks corresponding to the hBN E_{2g} and Si 3rd order TO modes.

AFM height data taken from a sample with mono and bi-layer thick hBN is shown in Fig. S4. Line scans across six different mono- to bi-layer steps show height differences from 0.3 to 0.38nm. Within experimental uncertainties, these height variations are consistent with the known van der Waals separation between two hBN atomic layers.

AFM height data taken from a sample with mono-, bi-, and tri-layer thick hBN is shown in Fig. S5. Line scans across these steps show mono- to tri-layer step heights ranging from 0.64 to 0.71 nm, and bi to tri-layer step heights from 0.31 to 0.34 nm. These values are consistent with van der Waals separation between the third and the second hBN layer, as well as between the second and the first hBN layer.
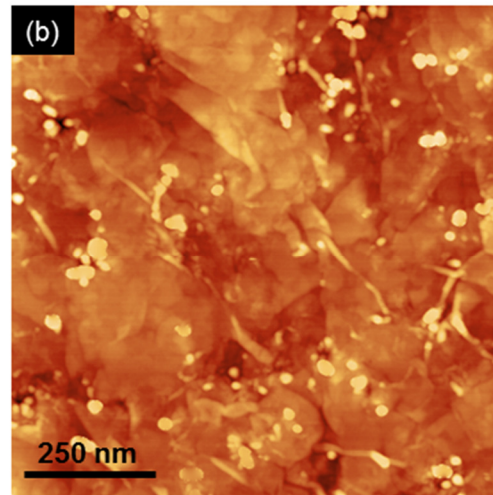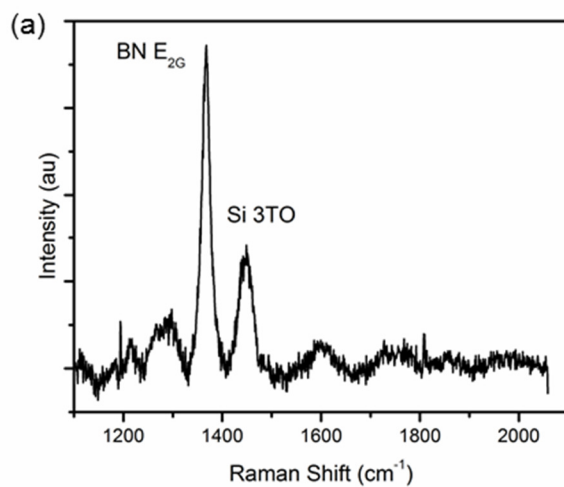
Figure S3. (a) Raman spectrum and (b) AFM height map from hBN film grown for 60 min.
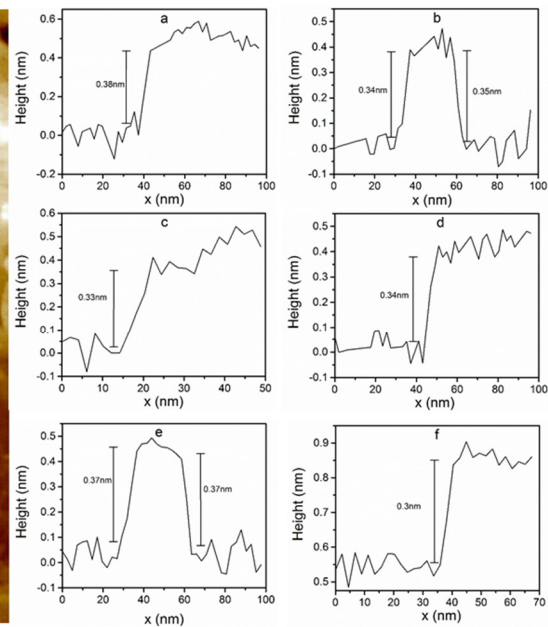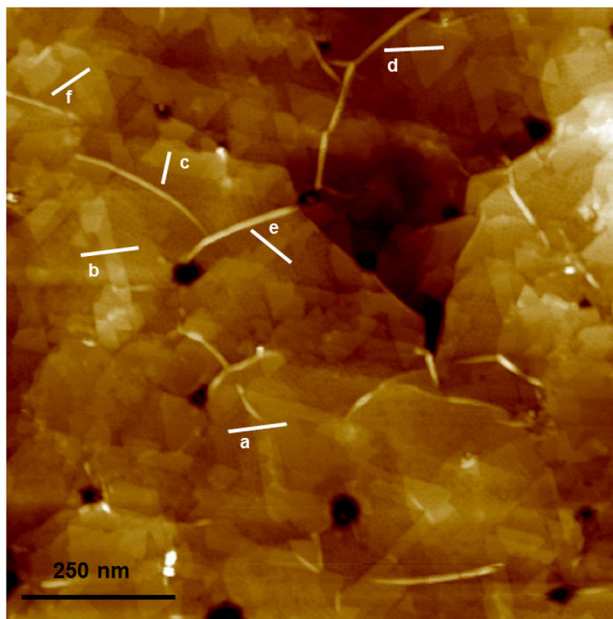

Figure S4. AFM height contrast showing hBN mono- and bilayers. Six line scans (a through f) are shown on the right.
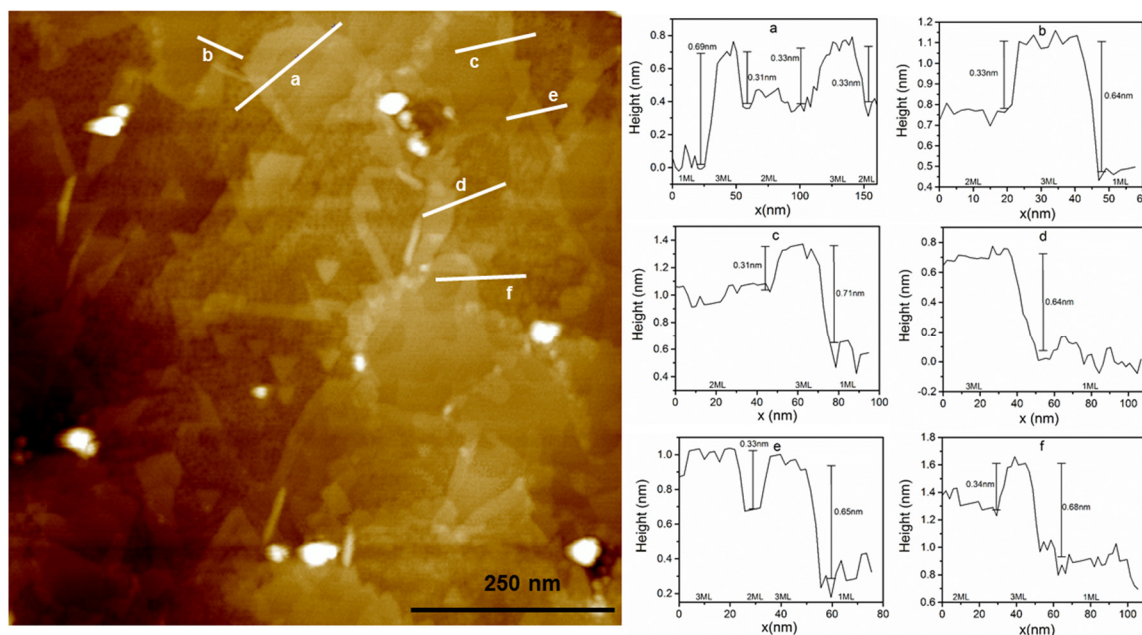
Figure S5. AFM height contrast showing mono-, bi-, and trilayers of hBN. Six line scans (a through f) are shown on the right.

4. Thermodynamic arguments in favor of six-atom ring formation

There are general thermodynamic arguments in favor of ring formation and of molecular hydrogen in the deposition of TEB and ammonia on Cu or hBN/Cu. Using standard dissociation energy of various bonds at room temperature [1], we can assess at least qualitatively the propensity of a system consisting of ammonia and TEB radicals to form B-N bonds. The bond energies of various bonds that can form in this system are as follows [1]:

B-B (297 kJ/mol) < B-H (331 kJ/mol) < N-H (356 kJ/mol) < B-N (389 kJ/mol) < H-H (435 kJ/mol).
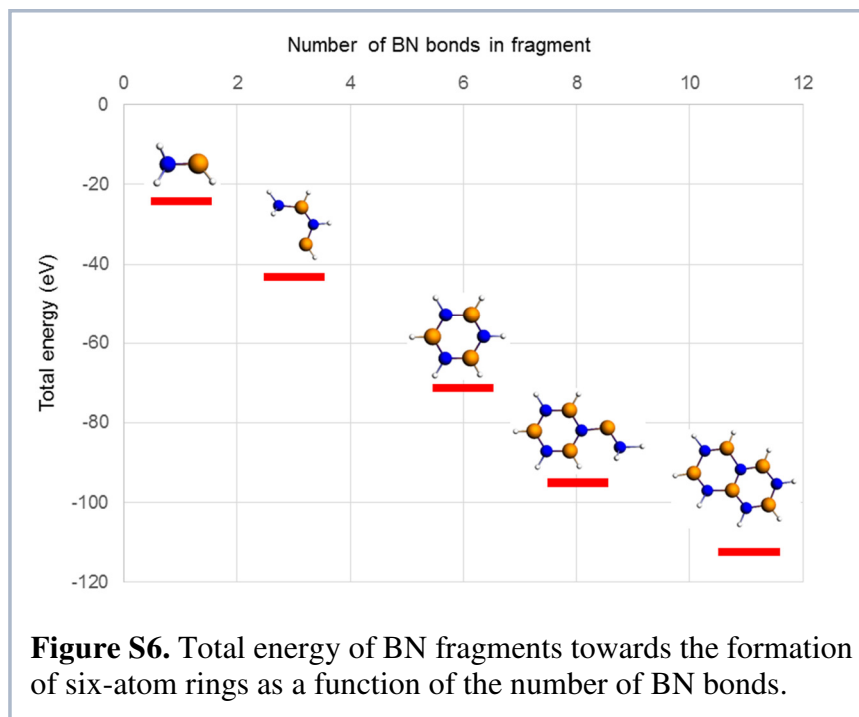
This sequence of inequalities shows a strong thermodynamic propensity for the formation of H_2 molecules (which diffuse away from the system), and of BN bonds. As seen above, the B-N bonds are favored over B-B, B-H, and N-H bonds –all of which have lower dissociation energies, i.e. they are weaker than B-N. In other words, based on these bond dissociation energies, the system would prefer to form the bonds that are harder to dissociate, i.e. the B-N and H_2 bonds.

In order to verify this prediction obtained from comparing standard bond strengths corresponding to bonding in simple molecules, we have also performed orbital-based density functional theory calculations with the ADF package [2]. We have chosen structures with increasing number of BN bonds. The rationale for choosing these structures with increasing number of BN units is to follow the stability (as described by the total energy) as a function of the size of 2-D BN "cluster" or fragment. The results are depicted in Fig. S6 for a sequence of selected structures. Following the

5

chart in Fig. S6, the H_2N-BN complexes could polymerize to create H_2N-BH-NH-BH, and then subsequently rings ($H_6N_3B_3$) and fused rings ($H_8N_5B_5$) on the surface.

These calculations show that the thermodynamic propensity for forming B-N bonds manifests itself in a marked decrease of the total energy of these structures (or fragments) with the number of B-N bonds in the fragment.

We have also done calculations with the same number of atoms but different bonding configurations between them, thus verifying that BN bonds are favored to form in a cluster with prescribed atomic composition.

Figure S6. Total energy of BN fragments towards the formation of six-atom rings as a function of the number of BN bonds.

These thermodynamic arguments are consistent with others in the literature, e.g., Ref. [3]. In Ref [3], the authors also create a pathway towards BN bonds and six-atom ring formation, and then determine that energies of the intermediates are lowest along that pathway. This is also consistent with the simple reasoning based on bond dissociation energies.

We note that these thermodynamics arguments are important, but, by themselves are not sufficient for determining pathways towards the formation of 2-D hBN layers, or flakes, or even six-atom rings. For this reason, we have performed direct molecular dynamics simulations to assess if the energy barriers encountered in the formation of various fragments are indeed surmountable at the relevant experimental temperatures. These are discussed in the main text.

References

[1] deB. Darwent, B., *Bond Dissociation Energies in Simple Molecules,* National Bureau of Standards, Nat. Stand. Ref. Data Ser. NSRDS-NBS 31 (1970).

[2] ADF2013, SCM, Theoretical Chemistry, Vrije Universiteit, Amsterdam, The Netherlands, http://www.scm.com; te Velde, G, Bickelhaupt, F.M., van Gisbergen, S.J.A., Fonseca Guerra, C., Baerends, E.J., Snijders, J.G., and Ziegler, T. , *Journal of Computational Chemistry*, **2001**, 22, 931.

[3] Park, S., Lee, J., Kim, H.S., Park, J.-B., Lee, K. H., Han, S. A., Hwang, S., Kim, S.-W., and Shin, H.-J., *ACS Nano*, **2015**, 9, 633–638.